

# Prediction of a Soil-Water Characteristic Curve Using a Genetic-Based Neural Network

A. Johari<sup>1</sup>, G. Habibagahi\* and A. Ghahramani<sup>1</sup>

In this paper, a Genetic-Based Neural Network (GBNN) is employed to predict the soil-water characteristic curve of unsaturated soils. A three-layer network has been trained by genetic algorithm and its topology is determined by trial and error. The network has five input neurons, namely, initial void ratio, initial gravimetric water content, logarithm of suction normalized with respect to air pressure, clay fraction and silt content. The network has five neurons in the hidden layer and the only output neuron is the gravimetric water content corresponding to the assigned input suction. Results from pressure plate tests carried out on clay, silty clay, sandy loam and loam, compiled in SoilVision software, was adopted as a database for training and testing the network. For this purpose, and after data digitization, a computer program coded in visual basic was developed and used for the analysis. Finally, neural network simulations are compared with the experimental results, as well as models proposed by other investigators. The comparison indicates the superior performance of the proposed method for predicting the soil-water characteristic curve.

## INTRODUCTION

Limitations in describing the mechanical behavior of unsaturated soils, based on a single effective stress equation similar to the one proposed by Bishop and Donald [1], have led to developing different approaches for modeling the observed behavior of these soils. The engineering behavior of unsaturated soils can be interpreted in terms of two different stress states, namely a net normal stress ( $\sigma - u_a$ ) and matric suction ( $u_a - u_w$ ). When soil behavior is related to these stress states, it is possible to propose more rational engineering design procedures. The Soil Water Characteristic Curve (SWCC), also known as the soil water-retention curve, is an important part of any constitutive relationship for unsaturated soils. SWCC, for an unsaturated soil, defines the relationship between water content and the corresponding suction.

SWCC can be considered as a continuous sigmoidal function describing the water storage capacity of a soil as it is subjected to various soil suctions. It

also includes important information about the amount of water contained in the pores at any soil suction and the pore size distribution corresponding to the stress state in the soil. SWCC and the unsaturated coefficient of permeability functions are required for solving transient water and solute transport problems associated with the vadose zone. Unsaturated soil behavior, such as shear strength, volume change, diffusivity and absorption, as well as most soil properties such as specific heat, permeability and thermal conductivity, can also be related to the soil water characteristic curve [2].

In this paper, GBNN is proposed for estimating the soil water characteristic curve using basic soil properties such as grain size distribution, initial void ratio, initial water content and the logarithm of suction, normalized with respect to atmospheric air pressure.

## AVAILABLE METHODS FOR DETERMINING SWCC

Several methods are available for predicting the SWCC of a particular soil. These are based on grain size distribution and other soil properties. These methods can be classified into four major groups described below:

---

1. *Department of Civil Engineering, Shiraz University, Shiraz, I.R. Iran.*

\*. *Corresponding Author, Department of Civil Engineering, Shiraz University, Shiraz, I.R. Iran.*

1. In the first group, water content at each suction value is correlated to the soil properties, such as grain size distribution and porosity. Generally, in this process, a regression analysis is required followed by a curve fitting procedure. Among important contributions to this group are the works of Visser [3], Gupta and Larson [4], Rawls and Brakensiek [5], Hutson and Cass [6], Williams and Ahuja [7], Reddi and Poduri [8], Tinjum et al. [9] and Mbagwu and Mbah [10];
2. Methods in the second group propose correlations between parameters of an assumed empirical equation for SWCC and the basic soil properties, such as grain size distribution and dry density, using a regression analysis. Among important contributions are the works of Williams et al. [11], Cresswell and Paydar [12] and Tomasella and Hodnett [13];
3. The third group involves physico-empirical modeling of SWCC. This converts the grain size distribution into a pore size distribution, which, in turn, is related to a distribution of water content and the associated pore pressure. Among important contributions are the works of Arya and Paris [14], Havercamp and Parlange [15], Smettem and Gregory [16], Fredlund et al. [17], Zapata et al. [18], Simms & Yanful [19], Aubertin et al. [20];
4. Artificial intelligence methods, such as neural network, genetic programming and other machine learning methods, have recently formed the fourth group. No significant attempt on this subject is cited in the literature so far.

In the following sections, fundamentals of the neural network and genetic algorithm, which are essential components for the proposed GBNN, are described in more detail.

## NEURAL NETWORK MODELING

A Neural Network (NN) is a computer-based modeling technique for computation and knowledge representation inspired by the neural architecture and operation of the human brain. NNs have experienced a considerable resurgence of interest in recent years, though they were initially developed during the early 1940s.

An Artificial Neural Network (ANN) is constructed directly from experimental data, a fundamentally different approach to model material behavior and, because of their ability to learn and generalize interactions among many variables, ANNs have the potential to model various aspects of material behavior. The basic architecture of ANN has been covered by Rumelhart & McClelland [21]. NN consists of a large number of highly interconnected processing units. Each processing unit (neuron), acting as an idealized

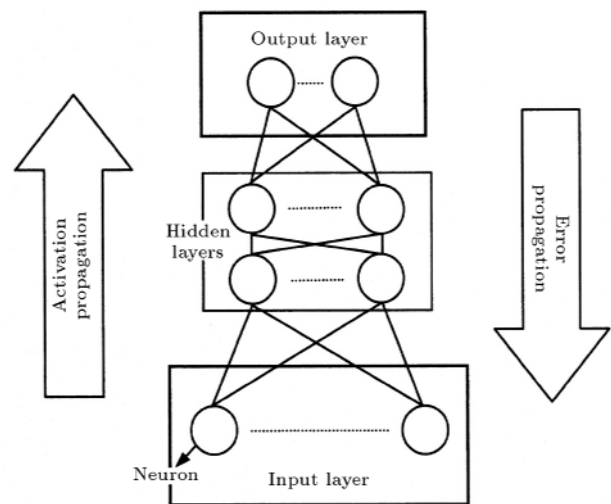


**Figure 1.** A typical ANN [22].

neuron in the human brain, receives input from the units to which it is connected, computes an activation level and transmits that activation to other processing units (Figure 1).

A multi-layer perceptron NN has an input layer, an output layer and a number of hidden layers connected to each other, as illustrated in Figure 1. Weights are assigned to the connections between these units. The presence of hidden layers allows the networks to represent and compute more complicated associations between input and output patterns.

A multi-layer feed forward ANN must be trained first and tested afterwards. During training, weights are adjusted in an iterative process. Activation propagation takes place in a feed-forward manner, from input to output layers. Conventionally, error (the difference between the network output and their target values) is back-propagated through the network and the weights are adjusted using a gradient descent rule. With the successful completion of the training, the iterative process reduces the error measure to a minimum and the collection of connection weights is captured. Such a neural network is ready to be used. When presented with an input pattern, a feed-forward network computation results in an output pattern that is the result of the generalization and synthesis of what it has learned and stored in its connection weights. The drawback of Back Propagation Neural Network (BPNN) is that there is a chance for the search to be trapped in local minima during error minimization and the algorithm may fail to capture the global minimum of the error function. To overcome this deficiency, a genetic algorithm is employed in this study to minimize the error function. This method has the powerful capability of capturing the global minimum. Details are explained in the following section.

## GENETIC ALGORITHM

A Genetic Algorithm (GA) is a statistical method for optimization and also searching. The characteristics of this algorithm prevent one from calling it a simple accidental searcher. The idea of this method, which was inspired by the theory of natural evolution, was first offered by Holland [23]. One important feature of GA is its durability and adaptability, since it provides a flexible balance between effectiveness and necessary characteristics for survival in different environments and under different conditions. Besides, if the adaptability of a system increases, it will be able to function longer and more effectively [24].

Searching in this algorithm is usually done with a group or population of binary or real strings, which are included in the form of the decision variable. Each string is analogous to a chromosome and each binary or real bit is analogous to a gene on that chromosome. There are three operations used in a simple GA: Selection, crossover and mutation.

### Selection

First, the objective function (fitness function) is evaluated for each string. Selection occurs when the individuals with higher fitness values are assigned higher probabilities of producing offspring for the next generation. Therefore, highly fit chromosomes will have a larger number of copies in the succeeding generation.

There are several different types of selection used in GA, such as Roulette-Wheel selection, Tournament and Ranking. The first method uses probability based on the fitness of the individual. If  $f(S_i)$  is the fitness of the solution  $i$  and  $\sum_{i=1}^m f(S_i)$  is the total sum for all the members of the population, then, the probability that the solution will be copied to the next generation is:  $f(S_i) / \sum_{i=1}^m f(S_i)$ , where  $S_i$  is the solution based on individual (member)  $i$ .

In the second method, a random number of solutions are taken from the population. The solution with the higher fitness will win. This process is repeated until the new population size is equal to the old population size. In rank selection as the third method, selection is based on sorting the fitness values of the solutions of the population. Probability of selection is proportional to fitness, where the worst will have a probability of 0 and the best will have a probability equal to 1.

### Crossover

After selection, crossover takes place. This operation works on one pair of chromosomes and can be performed in the form of “single-point crossover”, “two-

point crossover” or “uniform crossover”. It should be mentioned that the effect of each type of crossover on the convergence rate of the algorithm is not exactly determined and it depends on the problem at hand. Basically, this operation does not operate on all chromosomes of the population, since, if it did so, there would be a high probability that the population would lose certain characteristics. For this reason, the user specified probability ( $P_c$ ) is mated by randomly selecting place(s) to divide the two chromosomes and then exchanging the pieces.

### Mutation

In some cases, accidental changes, which are rare, occur in the environment. Although, in most cases, these changes (mutations) cause pre-term death of the mutants, in some cases, these mutations are considered as a success. In this algorithm, mutation randomly switches a bit or bits in the chromosomes with the user specified probability ( $P_m$ ) after crossover. This specified probability in every case is very small and even considered less than 0.05. By the influence of this operator, if the original bit were zero, it would change to one and, if it were one, it would change to zero. Using these operations, more fit members of the population are created over time and population evolves to optimal or near optimal solutions. Figure 2 shows the structure of a simple genetic algorithm.

## APPLICATION OF GA IN TRAINING NEURAL NETWORKS

Based on the features of the GA, it can be used for determining the optimal weights and also shape (topology) of a NN. In ordinary NNs, the “back propagation law” is used as a device for determining the minimum of function with weight variables connecting

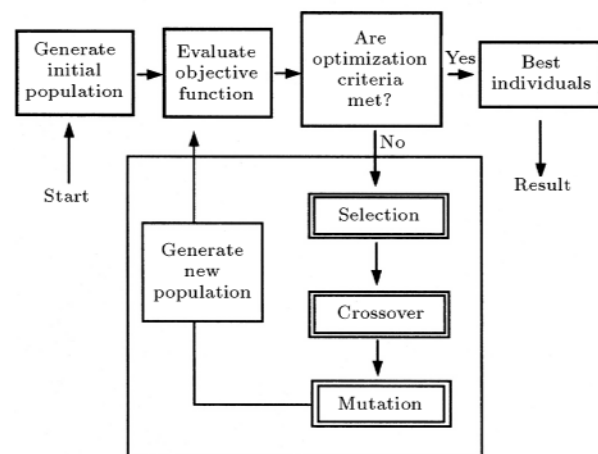


**Figure 2.** Structure of a single population evolutionary GA.

the layers. The logic of this law in multi-dimensional space, which has numerous extremum, is like the movement of a moving object that starts moving from a point in this space. In spite of having different devices in this method for preventing the moving object from situating in the local minimum, experience has shown that this is not always improbable. While, in using the GA, the starting point of movement in this space is from different points (equal to the number of the population), reaching to the absolute minimum is, therefore, more probable.

The error function ( $E$ ) is defined as:

$$E = \frac{1}{P} \sum_{P=1}^P [(O_p) - (T_p)]^2, \tag{1}$$

where  $T_p$  is the target value for the pattern ( $p$ ) and  $O_p$  is the output value of network, given by:

$$O_p = \sum_{j=1}^{N_h} w_{jk} \sum_{i=1}^{N_i} w_{ij} I_i^p, \tag{2}$$

in which:

- $W_{jk}$  weights between hidden and output layers,
- $W_{ij}$  weights between input and hidden layers,
- $I_i^p$  input variable  $i$  for pattern ( $p$ ),
- $N_i$  number of input neurons,
- $N_h$  number of hidden neurons.

Since GA is an algorithm that maximizes the objective function, in order to minimize the error function, the objective function is defined as:

$$F = \frac{1}{E}, \tag{3}$$

where  $E$  is the error function defined by Equation 1.

**Database**

Results from pressure plate tests on clay, silty clay, sandy loam and loam soil reported by different researchers and compiled by SoilVision [25] were adopted for the analysis. Table 1 indicates the range of basic soil properties adopted for this study. This database consists of the results from 186 pressure plate tests, together with their grain size distributions. Final

suction values were mostly in the range of 800 to 1700 kPa with few tests having suction values as large as  $10^5$  kPa. The results reported on these specimens were then digitized to obtain the necessary database. For digitization, an increasing incremental value of suction was adopted. Hence, the suction value was doubled in each increment. Initial suction value was fixed at 0.2 kPa. The database thus developed had a total number of 2694 patterns. For normalization, each component of the data set was normalized to lie in an interval of [0,1] using a max-min approach.

**APPLICATION OF GBNN FOR PREDICTION OF SWCC**

A computer program coded in visual basic for training the network by GA was developed. Five parameters, namely, void ratio, initial water content, logarithm of suction normalized with respect to air pressure [ $\log(Ua - Uw)/p_a$ ], clay fraction and silt content were selected as the input neurons. The output neuron yields the gravimetric water content corresponding to the assigned input suction. To find the optimum number of hidden neurons, they were decreased from a maximum of 10 neurons while checking the error measure of the network. This resulted in a total number of six neurons for the hidden layer. The optimum neural network structure had the following characteristics:

- Input neurons: Initial void ratio, Initial gravimetric water content,  $\log(\text{suction}/p_a)$ , clay fraction, silt content and one bias neuron ( $p_a$  is the atmospheric air pressure);
- Output neuron: Gravimetric water content;
- Number of hidden neurons: 5 neurons plus a bias neuron;
- Selection method: Roulette-Wheel.

Figure 3 shows the proposed network configuration.

After the current population, plus all the new children, has been formed, the program enters into a new phase. In this phase, a number of individuals are chosen to form a new population. In the coded subroutine, the best individual from both parents and children is kept in the new population

**Table 1.** Range of basic soil properties of specimens from SoilVision [25] for training model.

Void ratio: 0.458-2.846	Suction range (kPa): 0.2-104857.6
Specific gravity: 2.28-2.92	Clay (< 0.005 mm) (%): 4.4-76.7
Dry density (kg/m <sup>3</sup> ): 702-1811	Silt (0.005 mm-0.075 mm) (%): 10.3-87.5
Water content range (%): 0.18-98.27	Sand (> 0.075 mm) (%): 0.1-55.3
Initial water content (%): 17.34-105.41	



set and all 55 tests in the testing set. Figures 5 and 6 compare predicted gravimetric water content with the actual data for training and testing datasets, respectively. These figures show a good correlation between the predictions made using NN modeling and the actual data for both training and testing data.

### Comparison with Previous Works

As stated before, a number of methods have been presented by different investigators for estimating SWCC. Among these methods, the approach presented by Fredlund et al. [17] is considered to give a more reasonable estimate of the SWCC [18,27]. Therefore, in this paper, the proposed model is compared to the approach proposed by Fredlund et al. [17]. Fredlund et al. [17] estimated SWCC from the grain size distribution curve and volume mass properties. The procedure, as described in SoilVision software, consists of the following five stages:

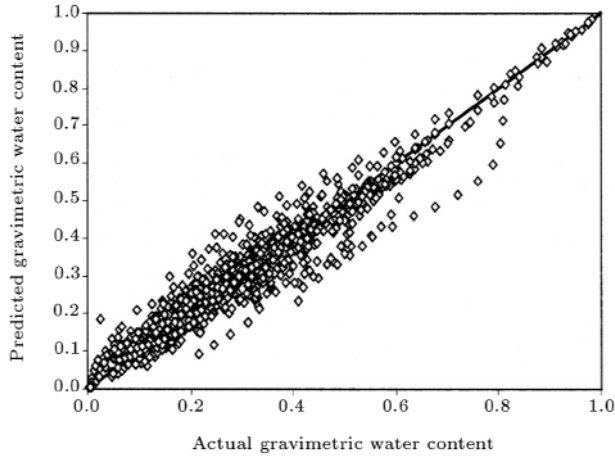


**Figure 5.** Actual versus predicted GWC for training model data in GBNN ( $R^2 = 0.94$ ).

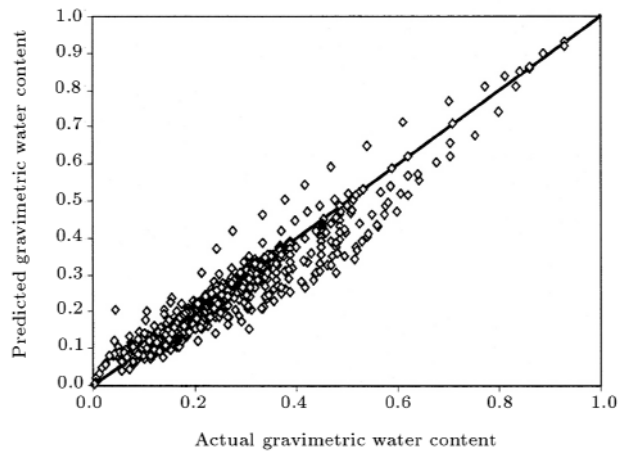


**Figure 6.** Actual versus predicted GWC for testing data in GBNN ( $R^2 = 0.91$ ).

1. Trends in the “ $n$ ” and “ $m$ ” parameters are determined by fitting the following equation to the available dataset:

$$\theta_w = \theta_s \left( 1 - \frac{\ln(1 + \psi/\psi_r)}{\ln(1 + 1000000/\psi_r)} \right) \left[ \frac{1}{\ln(e + (\psi/a)^n)} \right]^m, \quad (5)$$

where:

- $\Psi$  total soil suction (kPa),
- $e$  natural number, 2.71828,
- $\Psi_r$  total suction (kPa) corresponding to the residual water content,  $\theta_r$ ,
- $a$  a soil parameter, which is related to the air entry value of the soil (kPa),
- $n$  a soil parameter, which controls the slope at the inflection point in the SWCC,
- $m$  a soil parameter, which is related to the residual water content of the soil.

2. A unimodal or bimodal equation is used for fitting the grain size distribution curve. Therefore, the grain size has a continuous fit and proper definition of the extremes of the curve. Then, the grain size distribution is divided into small groups of uniformly size particles. An effective grain-size diameter is calculated for each grain-size curve segment, based on an equation of Vukovic and Soro [28] given by:

$$\frac{1}{d_e} = \frac{3}{2} \frac{\Delta g_l}{d_l} + \sum_{i=2}^{i=n} \frac{\Delta g_i}{d_i}, \quad (6)$$

where:

- $d_l$  largest diameter of the last fraction of the material,
- $g_l$  weight of the material of the last finest fraction in parts of total weight,
- $d_e$  effective grain diameter,
- $n$  total number of fraction.

3. The effective grain-size diameter is then plotted against the “ $n$ ” and “ $m$ ” parameters. The “ $n$ ” and “ $m$ ” parameters are determined for each soil by fitting laboratory data with a least-squares regression algorithm;
4. A packing porosity,  $n_p$ , is estimated using a neural network trained on a SoilVision dataset using 653 developing model data and 72 testing data, for each fraction. From packing porosity a void volume and then an effective grain diameter ( $d_e$ ) are calculated;

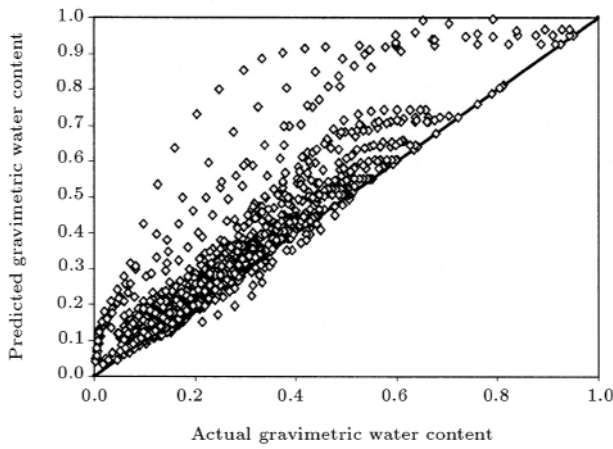


**Figure 7.** Actual versus predicted GWC for training model data using Fredlund et al. approach ( $R^2 = 0.85$ ).

5. From an effective grain diameter for each fraction and each fitted curve in Stage 3, the “ $m$ ” and “ $n$ ” parameter are determined and the SWCC is predicted for that segment. In this estimation, parameter “ $a$ ” was kept constant at 100 kPa;
6. The whole SWCC is finally generated by putting together these segments.

Figures 7 and 8 compare predicted gravimetric water content by Fredlund et al. [17] modeling with the actual data for training and testing, respectively.

Table 3 presents the error in neural network prediction compared with the aforementioned approach. In this table, the average relative error is defined as:

$$\text{Average relative error} = \frac{1}{N} \sum_{i=1}^N \left| \frac{A_i - P_i}{A_i} \right| \times 100,$$

and the mean sum squared of the error is defined by:

$$\text{MSSE} = \frac{1}{N} \sum_{i=1}^N (A_i - P_i)^2,$$

where:

- $A_i$  actual value for data  $i$ ,
- $P_i$  predicted value for data  $i$ ,
- $N$  total number of data available in the database.

From Table 3 it can be concluded that the proposed GBNN has a good capability to simulate the SWCC.

In order to show the robustness of the proposed method, simulation results were also compared on a one-to-one basis. Figures 9 to 11 show SWCC for 3 specimens used in training the model. In these figures, GBNN prediction and prediction based on the method suggested by Fredlund et al. [17] are compared with the experimental results. From these figures, it may be concluded that the proposed GBNN has a good potential for predicting SWCC with reasonable accuracy. Similarly, Figures 12 to 14 present the prediction of GBNN for 3 typical test specimens. From these figures, it may also be concluded that the proposed method is also capable of simulating new test results, though not as good as tests used in the training phase. The test results used to measure the performance of the proposed GBNN model correspond, respectively,

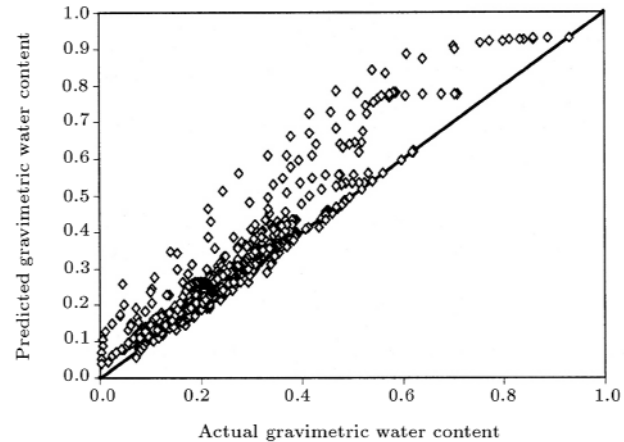


**Figure 8.** Actual versus predicted GWC for testing data using Fredlund et al. approach ( $R^2 = 0.89$ ).

**Table 3.** Comparing performance of GBNN with Fredlund et al. approach [17].

	Training Data		
	Average Relative Error (%)	MSSE	$R^{2*}$
Neural Network	12.94	0.0014	0.94
Fredlund et al. Approach [17]	34.73	0.0071	0.85
	Testing Data		
	Average Relative Error (%)	MSSE	$R^2$
Neural Network	14.26	0.0019	0.91
Fredlund et al. Approach [17]	35.39	0.0047	0.89

\*:  $R^2$  is the correlation coefficient (square of the Pearson product moment correlation coefficient)

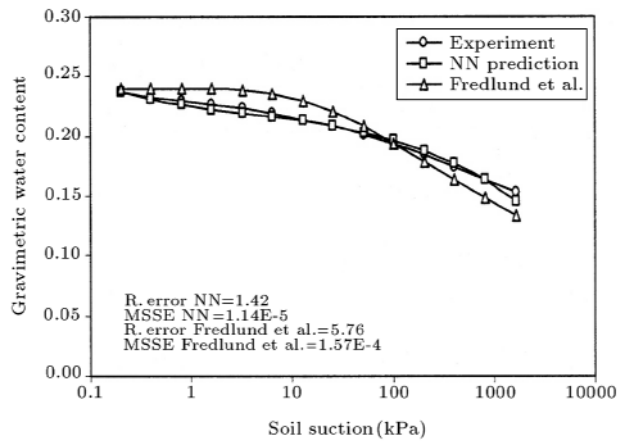


**Figure 9.** Best simulation results among tests used for training GBNN model (void ratio: 0.66, initial water content: 24.05%, clay content: 46.23%, silt content: 51.20%).

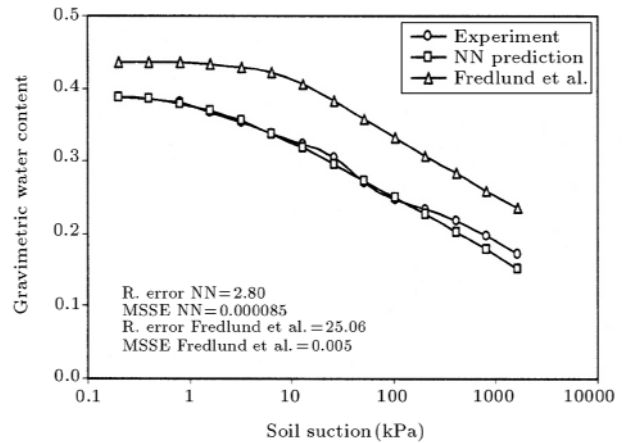


**Figure 12.** Best simulation results among tests used for testing GBNN model (void ratio: 1.16, initial water content: 43.59%, clay content: 40.04%, silt content: 48.33%).

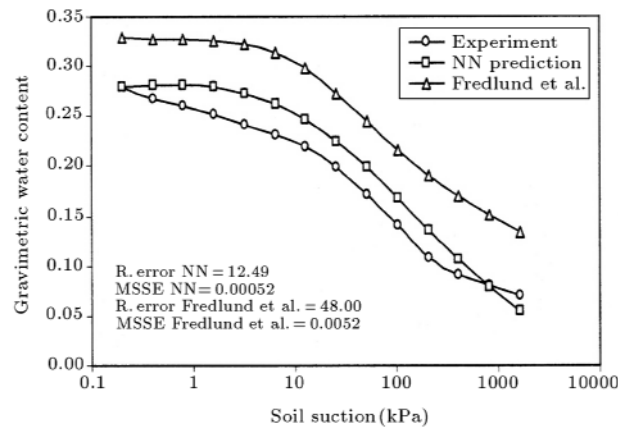


**Figure 10.** Average simulation results among tests used for training GBNN model (void ratio: 0.89, initial water content: 32.89%, clay content: 18.43%, silt content: 79.66%).

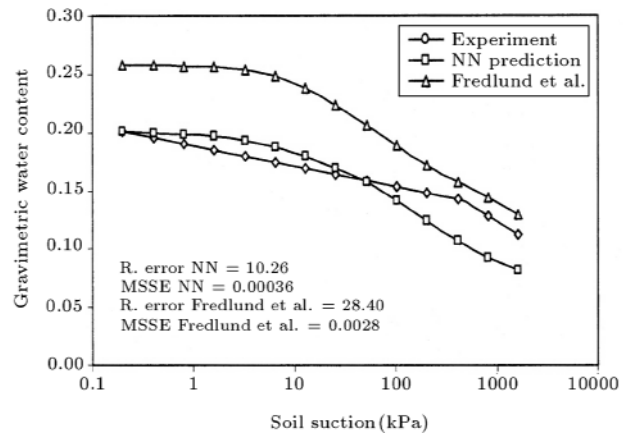


**Figure 13.** Average simulation results among tests used for testing GBNN model (void ratio: 0.70, initial water content: 25.74%, clay content: 29.79%, silt content: 54.29%).

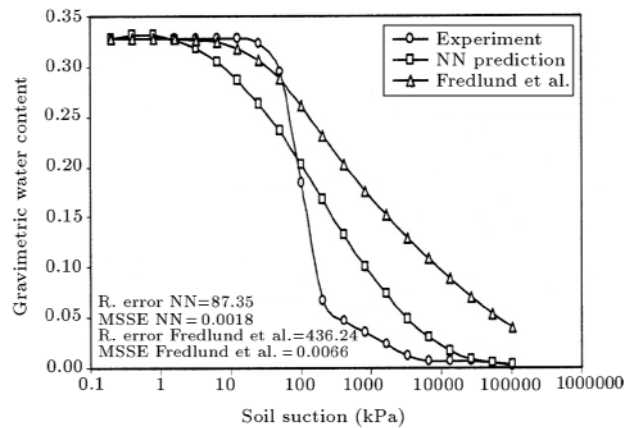


**Figure 11.** Worst simulation results among tests used for training GBNN model (void ratio: 0.96, initial water content: 32.9%, clay content: 21.86%, silt content: 77.41%).

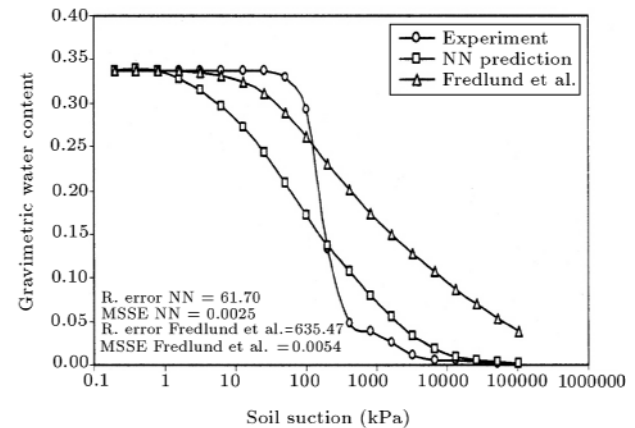


**Figure 14.** Worst simulation results among tests used for testing GBNN model (void ratio: 0.96, initial water content: 33.79%, clay content: 18.99%, silt content: 80.31%).



to the best, average and worst simulations among the training model and testing data sets. These results indicate the robust feature of the GBNN to learn and predict the SWCC without making any assumption or simplification a priori.

**Sensitivity Analysis**

To evaluate the model response to a change in input parameters, a parametric study was carried out. For this purpose, a typical specimen with basic soil properties given in Table 4 was assumed. In order to evaluate the influence of each parameter, one parameter was changed within a range of  $\pm 5\%$  or  $\pm 10\%$ , while keeping other parameters constant. Figures 15 through 18 indicate the results of this parametric study. Figure 15 indicates the influence of the clay fraction, while silt content was varied accordingly to keep sand content unchanged. As expected, with an increase in the percent of clay content, the SWCC shifts to the right indicating a higher suction required to drain the pores to certain water content. Figure 16 indicates the influence of clay fraction when the silt percent was constant. An increase in the percent of clay increases the fine percent of the soil and, therefore, a higher suction is required to drain the water from the soil, as predicted by GBNN. In Figure 17, silt fraction was varied and replaced by sand content, keeping constant the amount of the clay fraction. The prediction shows that a small change in silt percent did not considerably affect SWCC when it was replaced by sand. Figure 18

shows the influence of initial water content (or initial void ratio since the soil is almost fully saturated at very low suction values). The soil with a higher initial void ratio is more compressible compared to the same soil with a smaller void ratio. Hence, subjected to an increment of suction, the soil with a higher void ratio will lose more water compared with the same soil having a lower void ratio.

**CONCLUSION**

In ordinary NNs, the “back propagation of error” is used as an optimizing approach to determine the opti-

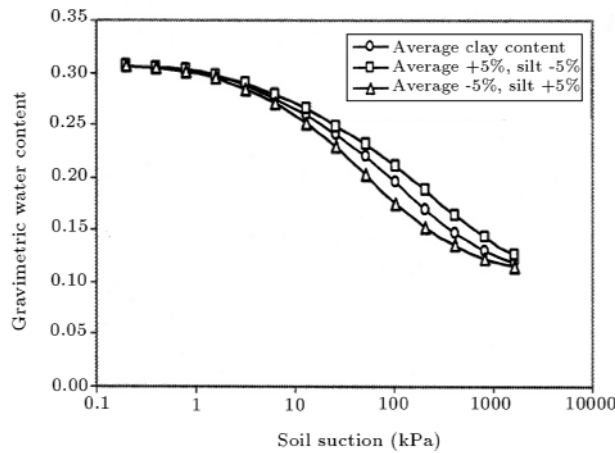


**Figure 15.** Influence of clay content on SWCC (fixed sand content).

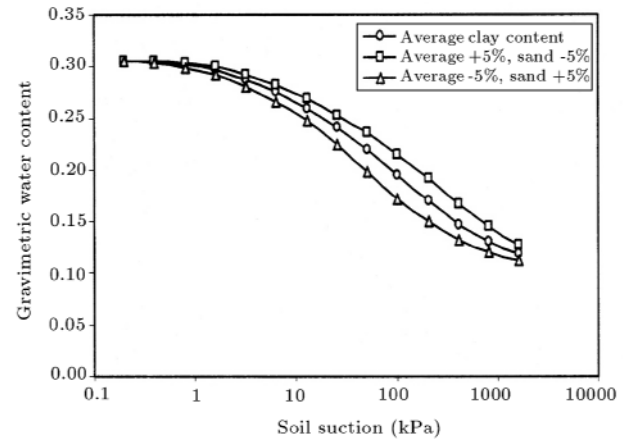


**Figure 16.** Influence of clay content on SWCC (fixed silt content).

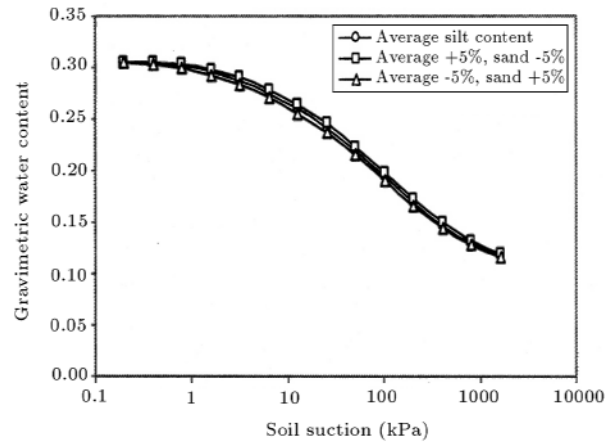


**Figure 17.** Influence of silt and sand content on SWCC (fixed clay fraction).

**Table 4.** Basic soil properties of specimen used for parametric study.

<b>Initial Void Ratio = 0.808</b>	<b>Initial Water Content (%) = 30.62</b>	<b>Dry Density = 1490.6 kg/m<sup>3</sup></b>
Clay (%) = 21.75	Silt (%) = 41.14	Sand (%) = 37.07
G <sub>s</sub> = 2.64		

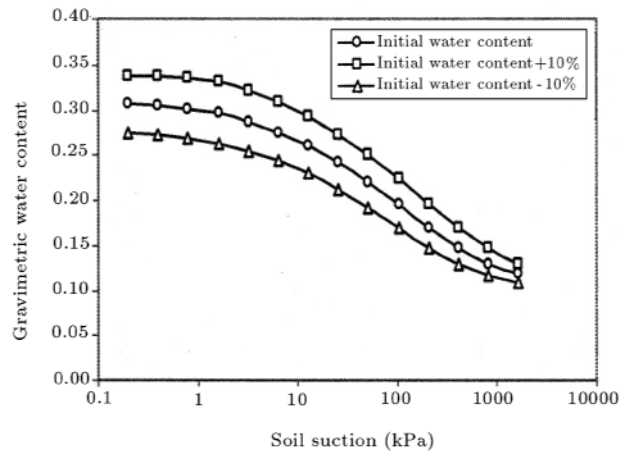


**Figure 18.** Influence of initial water content on SWCC.

imum weights connecting the layers. Despite different measures available to prevent trapping in local minima, experience has shown that this is not always successful. However, using GA as the training rule, function minimization starts from different points (equal to the population number) and, therefore, obtaining the absolute minimum is more probable. Indeed, the method is generally considered to give the global extremum. Hence, in this paper, GA was used to minimize the NN error function. A GBNN was developed to estimate the SWCC for unsaturated soils. A database containing the results of pressure plate tests carried out on a wide variety of fine grained soils and, thus, covering a wide range of soil properties was employed to develop the model. Test results were digitized and normalized to obtain the necessary database. During the first phase, the model was trained using the results from 131 pressure plate tests. In the second phase, the model was tested using 55 additional test results to which it had not been exposed during the first phase. The model prediction indicated a reasonable accuracy, both for the results used in the first phase, as well as in the testing phase. Furthermore, a parametric study of the model indicated the influence of various parameters such as clay content, silt percent, sand content and initial water content. The results indicated that clay content is the most important soil parameter. A small change in clay content (replaced by an equivalent amount of sand or silt) had a pronounced effect on the SWCC. However, it seems that opposite changes in silt or sand content (replacing sand with silt or vice versa) does not affect the SWCC appreciably. More studies are encouraged, especially in the following areas:

- Taking the hysteresis phenomena (wetting-drying cycle) into account,
- Determination of hydraulic conductivity of unsaturated soil from SWCC and its prediction by NN,
- Taking the influence of fabric, stress history and confinement into account.

## REFERENCES

1. Bishop, A.W. and Donald, I.B. "The experimental study of partly saturated soil in triaxial apparatus", *Proc., 5th Int. Conf. Soil Mech. and Found. Eng.*, **1**, pp 13-21 (1961).
2. Fredlund, D.G. and Rahardjo, H., *Soil Mechanics for Unsaturated Soils*, Wiley, New York, USA (1993).
3. Visser, W.C. "An empirical expression for the desorption curve", *Proc. of UNESCO IASH Symp. on Water in the Unsaturated Zone*, Netherlands, pp 329-335 (1969).
4. Gupta, S.C. and Larson, W.E. "Estimating soil water retention characteristics from particle size distribution, organic matter percent and bulk density", *Water Resources Res. J.*, **15**(6), pp 1633-1635 (1979).
5. Rawls, W.J. and Brakensiek, D.L. "Estimating soil water retention from soil properties", *J. of the Irrig. and Drain. Div., ASCE*, **108**(IR2), pp 166-171 (1982).
6. Hutson, J.L. and Cass, A. "A retentivity function for use in soil water simulation models", *Soil Sci J.*, **38**(1), pp 105-113 (1987).
7. Williams, R.D. and Ahuja, L.R. "Estimating soil water characteristic using measured physical properties and limited data", *Proc. of the Int. Workshop on Indirect Methods for Estimating the Hydraulic Properties of Unsaturated Soils*, California, USA, pp 405-416 (1992).
8. Reddi, L.N. and Poduri, R. "Use of liquid limit state to generalize water retention properties of fine-grained soils", *Geotech.*, **47**(5), pp 1043-1049 (1997).
9. Tinjum, J.M., Benson, C.H. and Blotz, L.R. "Soil water characteristic curves for compacted clays", *J. of Geotech. and Geoenviron. Eng.*, **123**(11), pp 1060-1069 (1997).
10. Mbagwu, J.S.C. and Mbah, C.N. "Estimation water retention and availability in Nigerian soils from their saturation percentage", *Communications in Soil Sci. and Plant Analysis*, **29**(7/8), pp 913-922 (1998).
11. Williams, J., Prebble, R.E., Williams, W.T. and Hignett, C.T. "The influence of texture, structure and clay mineralogy on the soil moisture characteristic", *Aust. J. of Soil Res.*, **21**, pp 15-32 (1983).
12. Cresswell, H.P. and Paydar, Z. "Water retention in Australian soil, description and prediction using parametric functions", *Aust. J. of Soil Res.*, **34**(2), pp 195-212 (1996).
13. Tomasella, J. and Hodnett, M.G. "Estimating soil water retention characteristics from limited data in Brazilian Amazonia", *Soil Sci. J.*, **163**(3), pp 190-202 (1998).
14. Arya, L.M. and Paris, J.F. "A physicoempirical method to predict the soil moisture characteristic from particle-size distribution and bulk density data", *Soil Sci. Soc. of America J.*, **45**, pp 1023-1030 (1981).
15. Havercamp, R. and Parlange, J.Y. "Predicting the water-retention curves from particle size distribution, sandy soils without organic matter", *Soil Sci. j.*, **142**(6), pp 325-339 (1986).

16. Smettem, K.R.J. and Gregory, P.J. "The relation between water retention and particle size distribution parameters for some predominantly sandy western Australian soil." *Aust. J. of Soil Res.*, **34**(5), pp 695-708 (1996).
17. Fredlund, M.D., Fredlund, D.G. and Wilson, G.W. "Prediction of the soil-water characteristic curve from grain size distribution and volume-mass properties", *Proc., 3rd Brazilian Symp. on Unsaturated Soils*, Rio de Janeiro, pp 13-23 (1997).
18. Zapata, C.E., Houston, W.N. and Walsh, K.D. "Soil-water characteristic curve variability", *Advances in Unsaturated Geotechnics*, Geotech. Special Pub., **99**, pp 84-124 (2003).
19. Simms, P.H. and Yanful, E.K. "Predicting soil water characteristic curves of compacted plastic from measured pore size distributions", *Geotech.*, **52**(4), pp 269-278 (2002).
20. Aubertin, M., Mbonimpa, M., Bussiere, B. and Chapuis, R.P. "A model to predict the soil retention curve from basic geotechnical properties", *Can. Geotech. J.*, **40**, pp 1104-1122 (2003).
21. Rumelhart, D.E. and McClelland, J.L., *Explorations in Parallel Distributed Processing*, The MIT Press, Boston, Massachusetts, USA (1988).
22. Ghaboussi, J., Garrett, Jr. and Wu, X. "Knowledge-based modeling of material behavior with neural networks", *J. of Eng. Mech., ASCE*, **117**(1), pp 132-153 (1991).
23. Holland, J.H., *Adaptation in Natural and Artificial System*, University of Michigan Press, Ann Arbor, MI, USA (1975).
24. Goldberg, D., *Genetic Algorithms in Machine Learning Optimization and Search*, Addison-Wesley, USA (1988).
25. *SoilVision*, SoilVision System Ltd., Sask., Saskatchewan, Canada (2002).
26. Pham, D.T. and Karaboga, D., *Intelligent Optimization Techniques*, Springer-Verlag, London, UK (2000).
27. Fredlund, M.D., Wilson, G.W. and Fredlund, D.G. "Use of grain-size distribution for estimation of the soil water characteristic curve", *Can. Geotech. J.*, **39**(5), pp 1103-1117 (2002).
28. Vukovic, M. and Soro, A., *Determination of Hydraulic Conductivity of Porous Media from Grain-Size Composition*, Water Resources Pub., Littleton, CO, USA (1992).